Kobe University Repository : Kernel

PDF issue: 2025-12-04

Interaction of nectin-2α with the auxiliary protein of the voltage-gated A-type K+ channel Kv4.2 dipeptidyl aminopeptidase-like protein at the boundary between the adjacent somata of…

Shiotani, Hajime ; Miyata, Muneaki ; Mizutani, Kiyohito ; Wang, Shujie ; Mizoguchi, Akira ; Mochizuki, Hideki ; Mandai, Kenji ; Takai, Yoshimi

(Citation)
Molecular and Cellular Neuroscience,94:32-40

(Issue Date)
2019-01

(Resource Type)
journal article

(Version)
Accepted Manuscript

(Rights)
© 2018 Elsevier B.V.
This manuscript version is made available under the CC-BY-NC-ND 4.0 license
http://creativecommons.org/licenses/by-nc-nd/4.0/

(URL)
https://hdl.handle.net/20.500.14094/90007127

Interaction of nectin-2α with the auxiliary protein of the voltage-gated A-type K^+ channel Kv4.2 dipeptidyl aminopeptidase-like protein at the boundary between the adjacent somata of clustered cholinergic neurons in the medial habenula

Hajime Shiotani[1, 2], Muneaki Miyata[1], Kiyohito Mizutani[1], Shujie Wang[3], Akira Mizoguchi[3], Hideki Mochizuki[2], Kenji Mandai[1, 4]*, and Yoshimi Takai[1]*

[1]Division of Pathogenetic Signaling, Department of Biochemistry and Molecular Biology, Kobe University Graduate School of Medicine, Kobe, Hyogo 650-0047, Japan

[2]Department of Neurology, Osaka University Graduate School of Medicine, Suita, Osaka 565-0871, Japan

[3]Department of Neural Regeneration and Cell Communication, Mie University Graduate School of Medicine, Tsu, Mie 514-8507, Japan.

[4]Department of Biochemistry, Kitasato University School of Medicine, Sagamihara, Kanagawa 252-0374, Japan

*Corresponding authors:

Yoshimi Takai MD, PhD

Division of Pathogenetic Signaling, Department of Biochemistry and Molecular Biology, Kobe University Graduate School of Medicine

1-5-6 Minatojima-minamimachi, Chuo-ku, Kobe, Hyogo 650-0047, Japan

E-mail: ytakai@med.kobe-u.ac.jp

Kenji Mandai MD, PhD

Department of Biochemistry, Kitasato University School of Medicine

1-15-1 Kitasato, Minami-ku, Sagamihara, Kanagawa 252-0374, Japan

E-mail: mandai@med.kitasato-u.ac.jp

ABSTRACT

The medial habenula (MHb) receives septal inputs and sends efferents to the interpeduncular nucleus and is implicated in stress, depression, memory, and nicotine withdrawal syndrome. We previously showed by immunofluorescence microscopy that the cell adhesion molecule nectin-2α is expressed in the cholinergic neurons in the developing and adult mouse MHbs and localized at the boundary between the adjacent somata of clustered cholinergic neurons where the voltage-gated A-type K^+ channel Kv4.2 is localized. We further showed by immunoelectron microscopy that Kv4.2 is localized at the membrane specializations (MSs) whereas nectin-2α is localized mostly outside of these MSs. In addition, we showed that genetic ablation of *nectin-2* delays the localization of Kv4.2 at the MSs in the developing MHb. We investigated here how nectin-2α regulates this localization of Kv4.2 at the MSs. *In vitro* biochemical analysis revealed that nectin-2α interacted with the auxiliary protein of Kv4.2 dipeptidyl aminopeptidase-like protein 6 (DPP6), but not with Kv4.2 or another auxiliary protein Kv channel interacting protein 1 (KChIP1). Immunofluorescence microscopy analysis showed that DPP6 was colocalized with nectin-2α at the boundary between the adjacent somata of the clustered cholinergic neurons in the developing and adult MHbs. Immunoelectron microscopy analysis on this boundary revealed that DPP6 was localized both at the inside and the outside of the MSs. Genetic ablation of *nectin-2* did not affect the localization of DPP6 at the boundary between the adjacent somata of the clustered cholinergic neurons in the developing and adult MHbs. These results indicate that nectin-2α interacts with DPP6 but regulates the localization of Kv4.2 at the MSs in a DPP6-independent manner.

Highlights

Nectin-2α interacted with DPP6, but not with Kv4.2 or KChIP1

Nectin-2α, Kv4.2, and DPP6 were expressed in the mouse medial habenula.

They were localized at the boundary between the somata of the clustered neurons.

Nectin-2α regulated the localization of Kv4.2 in a DPP6-independent manner.

Keywords

Nectin, Kv4.2, DPP6, cell adhesion, medial habenula, cholinergic neuron

1. Introduction

The habenula, consisting of the medial habenula (MHb) and the lateral habenula, is located in the dorsal end of the diencephalon and faces to the third ventricle (Fig. 1, A and B). The MHb receives afferents from the triangular septum and the medial septal complex (the medial septum and the nucleus of diagonal band) and extends efferents almost exclusively to the interpeduncular nucleus in the midbrain through the fasciculus retroflexus (Carlson et al., 2001; Herkenham and Nauta, 1977, 1979). The MHb responds to glutamate and γ-aminobutyric acid (GABA), which are produced in the triangular septum and in the medial septal complex, respectively (Qin and Luo, 2009). The neurons in the MHb release three neurotransmitters in the interpeduncular nucleus: acetylcholine, glutamate, and substance P (Carlson et al., 2001; Herkenham and Nauta, 1979). The interpeduncular nucleus extends efferents to the ventral tegmental area and the raphe nuclei and regulates dopamine and serotonin levels, respectively (Balcita-Pedicino et al., 2011; Cuello et al., 1978; Groenewegen et al., 1986). Thus, the MHb connects the basal forebrain with the midbrain nuclei and regulates the activities of these monoaminergic neurons (Christoph et al., 1986; Nishikawa et al., 1986; Nishikawa and Scatton, 1985; Wang and Aghajanian, 1977). The MHb is divided into five subnuclei: the superior part (MHbS), the ventral region of the inferior part (MHbI), the lateral part (MHbL), the dorsal region of the central part (MHbCd), and the ventral region of the central part (MHbCv) (Aizawa et al., 2012; Andres et al., 1999). The MHbS exclusively produces glutamate; the MHbCd produces both glutamate and substance P; and the MHbI, the MHbCv, and the MHbL produce both glutamate and acetylcholine (Aizawa et al., 2012). The MHb is implicated in stress, depression, memory, and nicotine withdrawal syndrome (Kobayashi et al., 2013; Mathuru and Jesuthasan, 2013; Molas et al., 2017; Shumake et al., 2003).

Nectin-2 is a member of the immunoglobulin-like cell adhesion molecule (CAM) nectin family, consisting of four members, which plays roles in cell adhesion, proliferation, differentiation, survival, and migration (Takai et al., 2008a; Takai et al., 2008b). Nectin-2, also named as poliovirus receptor related 2 or CD112, has two splice variants; a shorter variant nectin-2α and a longer variant nectin-2δ. Both the transcripts are expressed in the ubiquitous tissues and organs (Aoki et al., 1997; Eberlé et al., 1995). The amino acid sequences of the extracellular regions excluding the juxtamembrane region consisting of 12

amino acids are shared in these two mouse variants, whereas those of the other regions, including the juxtamembrane regions, the transmembrane regions, and the intracellular regions, are different between them (Eberlé et al., 1995). The *nectin-2* gene was originally cloned as a murine homolog of the poliovirus receptor gene (Morrison and Racaniello, 1992), but its gene product was later shown to serve as an entry receptor for herpes simplex virus (Warner et al., 1998). In humans, the *NECTIN2* gene was shown to be genetically associated with Alzheimer's disease (Harold et al., 2009; Logue et al., 2011; Takei et al., 2009).

It was previously shown that nectin-2α is expressed in both cultured mouse neurons and astrocytes whereas nectin-2δ is selectively expressed in cultured astrocytes (Miyata et al., 2016). In the mouse brain, nectin-2α and/or nectin-2δ (nectin-2α/δ) is highly concentrated in the pia mater, walls of the lateral ventricles, the choroid plexus, and the habenula in the forebrain. Nectin-2α/δ is concentrated also around the blood vessels weakly. Nectin-2δ, but not nectin-2α, is localized at the adhesion sites between adjacent cultured astrocytes, but, in the brain, it is localized on the plasma membrane of the perivascular astrocytic endfoot processes facing the basement membrane of blood vessels. Genetic ablation of *nectin-2* causes degeneration of perivascular astrocytic endfoot processes and neurons in the cerebral cortex during adulthood. These results uncovered for the first time the localization and functions of nectin-2 in the brain.

Subsequently, we showed that nectin-2α, but not nectin-2δ, is prominently expressed in the adult MHb (Shiotani et al., 2018) (Fig. 1, C and D). Nectin-2α is expressed in the cholinergic neurons in the developing and adult MHbs and localized both at the boundary between the adjacent somata of the clustered cholinergic neurons and in the synaptic regions. We focused on nectin-2α localized at the boundary between the adjacent somata of the clustered cholinergic neurons and investigated its detailed localization and role. It was previously shown that the membrane specializations (MSs) are observed at the boundary between the adjacent somata of the neurons in the MHb and that voltage-gated A-type K^+ channels, Kv4.2 and Kv4.3, are localized at the MSs of the clustered neurons (Kollo et al., 2006). Kv4.2 and Kv4.3 belong to the family of the voltage-gated A-type K^+ channel with rapid activation and inactivation, resulting in transient A-type K^+ current (Birnbaum et al., 2004). They are associated with two auxiliary proteins: Kv channel interacting protein

(KChIP) and dipeptidyl aminopeptidase-like protein (DPP) (An et al., 2000; Nadal et al., 2003). The physiological function of the MSs in the MHb remains unknown. The analysis by immunoelectron microscopy on this boundary revealed that Kv4.2 is localized at the MSs with plasma membrane darkening in an asymmetrical manner, whereas nectin-2α is localized on the apposed plasma membranes mostly at the outside of these MSs, but occasionally localized at their edges and insides (Shiotani et al., 2018). Nectin-2α at this boundary is not colocalized with the nectin-2α-binding protein afadin, other CAMs, or their interacting peripheral membrane proteins, suggesting that nectin-2α forms a cell adhesion apparatus different from the Kv4.2-associated MSs (Shiotani et al., 2018). In addition, genetic ablation of *nectin-2* delays the localization of Kv4.2 at the boundary between the adjacent somata of the clustered cholinergic neurons in the developing MHb (Shiotani et al., 2018). These results revealed the unique localization of nectin-2α and its regulatory role in the localization of Kv4.2 at the MSs in the MHb. However, it remains elusive how nectin-2α regulates the localization of Kv4.2 at the boundary between the adjacent somata of the clustered cholinergic neurons in the developing MHb. We showed here that nectin-2α interacted with DPP6, but not with Kv4.2 or KChIP1, but regulated the localization of Kv4.2 at the MSs in a DPP6-independent manner.

2. Materials and Methods

2.1. Mice

C57BL/6J mice were purchased from CLEA Japan (Tokyo, Japan). *Nectin-2*$^{-/-}$ (aka, *nectin2*^{tm1Smu}/*nectin2*^{tm1Smu}) and *nectin-2*$^{+/-}$ mice (Mueller et al., 2003; Ozaki-Kuroda et al., 2002) were maintained on a C57BL/6J background. The day of birth was defined as P0. All animal experiments were performed in accordance with the guidelines of the institution and approved by the administrative panel on laboratory animal care of Kobe University. This study was approved by the president of Kobe University after being reviewed by the Kobe University Animal Care and Use Committee (approval numbers: 24-03-04 and 30-07-01),

and animal experiments were conducted in accordance with the regulations for animal experimentation of Kobe University.

2.2. Constructs

The plasmid encoding N-terminally FLAG-tagged mouse nectin-2α (pFLAG-CMV1-nectin-2α) was constructed as described previously (Miyata et al., 2016). The plasmids encoding the mouse nectin-2α mutant lacking the cytoplasmic region, corresponding to amino acids 385–467 (pFLAG-CMV1-nectin-2α–ΔCP), and the nectin-2α mutant lacking the extracellular region, corresponding to amino acids 30–338 (pFLAG-CMV1-nectin-2α–ΔEC), were constructed by PCR and introduced into the pFLAG-CMV1 expression vector. The cDNAs encoding mouse Kv4.2 (GenBank accession number, NM_019697), mouse DPP6 (GenBank accession number, NM_207282), and mouse KChIP1 (GenBank accession number, NM_001190885) were cloned from the first strand cDNA. Total RNA from 10-day-old mouse brain was extracted using a QIAGEN RNeasy Plus Mini Kit (QIAGEN, Germantown, MD, USA; catalog number 74134) according to the manufacturer's protocol. The first strand cDNA was synthesized using a Super Script IV-First Strand Synthesis kit (Thermo Fisher Scientific, Waltham, MA) with random hexamer primers. The primer sets used for the cloning were listed: 5'-ATATCTTAAGATGGCAGCCGGTGTTGCAG-3' and 5'-AATTGCGGCCGCCAAGGCAGACACCCTGAC-3' for mouse Kv4.2; 5'-ATATGCTAGCATGGCTTCGCTGTACCAAAG-3' and 5'-AATTGCGGCCGCGTCCTCCTCCTCCTCCTC-3' for mouse DPP6; 5'-ATATGATATCATGGGGGCCGTCATGGG-3' and 5'-AATTGCGGCCGCCATGACATTTTGGAACAGC-3' for mouse KChIP1. These cDNAs were inserted into the modified pcDNA3.1 vector containing a 3 × hemagglutinin (HA) epitope sequence. Then, the expression vectors for C-terminally HA-tagged mouse Kv4.2 (pcDNA3.1-Kv4.2-HA), C-terminally HA-tagged mouse DPP6 (pcDNA3.1-DPP6-HA), and C-terminally HA-tagged mouse KChIP1 (pcDNA3.1-KChIP1-HA) were constructed.

2.3. Antibodies

Rat anti-nectin-2α/δ monoclonal antibody (mAb) was prepared as described previously (Takahashi et al., 1999). The antibodies (Abs) listed below were purchased from commercial sources: rabbit anti-FLAG-probe polyclonal antibody (pAb) (Sigma-Aldrich, St. Louis, MO; catalog number F7425); rabbit anti-HA-probe pAb (Santa Cruz Biotechnology Inc., Dallas, TX; catalog number sc-805); and rabbit anti-DPP6 pAb (Alomone Labs, Jerusalem, Israel; catalog number APC-146). For immunofluorescence microscopy, primary Abs were visualized using Alexa Fluor-conjugated goat secondary Abs (Thermo Fisher Scientific).

2.4. In vitro immunoprecipitation assay

HEK293E cells were transfected with various combinations of plasmids and cultured for 48 h. Then, the cells were lysed with a lysis buffer [50 mM Tris-HCl at pH 7.4, 140 mM NaCl, 1% TritonX-100, 1% sodium deoxycholate, 0.1% SDS, cOmplete Mini protease inhibitor cocktail tablets (Roche Diagnostics, Mannheim, Germany; catalog number 11836170001), and phosphatase inhibitor cocktail 3 (Sigma-Aldrich, catalog number P0044)] by standing on ice for 15 min. The lysates were then centrifuged at 100,000 × *g* at 4°C for 30 min. The supernatant was pre-cleared with protein G-Sepharose 4 Fast Flow beads (GE Healthcare Bioscience, Buckinghamshire, UK; catalog number 17-0618-02) at 4°C for 1 h. The pre-cleared lysates were incubated with FLAG-tagged protein purification gel (DDDDK-tagged protein purification gel, MBL, Nagoya, Japan; catalog number 3328) or HA-tagged protein purification gel (MBL, catalog number 3321) at 4°C for 3 h. After the gels were extensively washed with the lysis buffer, bound proteins were eluted by boiling the gels in SDS sample buffer for 5 min, and subjected to SDS-PAGE, followed by Western blotting using the indicated Abs.

2.5. Western blotting

The immunoprecipitates were subjected to SDS-PAGE and transferred to Immobilon-P polyvinylidene difluoride membranes (EMD Millipore, Billerica, MA). The membranes

were blocked in 1% non-fat dry milk, and then incubated with the primary Abs, followed by incubation with HRP-conjugated secondary Abs. The signals were visualized by incubation with Immobilon Western Chemiluminescent HRP Substrate (EMD Millipore, catalog number WBKLS0500), and then detected using the ImegeQuant LAS4000 (GE Healthcare Bioscience).

2.6. Immunofluorescence microscopy

Immunofluorescence microscopy was performed as described previously (Toyoshima et al., 2014). In brief, mice were deeply anesthetized and transcardially perfused at room temperature with 1 × Hanks' Balanced Salt Solution with Ca^{2+} and Mg^{2+} (HBSS; Thermo Fisher Scientific) containing 10 mM HEPES, 1 mM sodium pyruvate, 4% sucrose, heparin, and cOmplete Mini protease inhibitor cocktail tablets (Roche Diagnostics), followed by perfusion of 2% paraformaldehyde in the abovementioned HBSS based buffer. After dehydration with 30% sucrose in phosphate buffered saline, whole brains were embedded in OCT compound (Sakura Finetek, Tokyo, Japan). Cryostat sections were incubated at 62°C for 20 min in HistoVT One antigen retrieval solution (Nacalai Tesque, Kyoto, Japan; catalog number 06380-05) and then incubated with 1% bovine serum albumin, 10% normal goat serum, and 0.25% Triton X-100 in phosphate buffered saline at room temperature for 20 min. The sections were stained with the indicated Abs, and then with appropriate fluorophore-conjugated secondary Abs (1:600). Confocal image acquisition was performed on a C2 confocal laser-scanning microscope (Nikon, Tokyo, Japan) using a 20×/0.75 or 40×/0.95 objective lens (Plan Apo numerical aperture water immersion objective lens (Nikon)). Images captured on the C2 confocal laser-scanning microscope were analyzed using NIS Elements acquisition software (Nikon).

2.7. Immunoelectron microscopy

Immunoelectron microscopy was performed using a silver-enhanced immunogold method where 0.5% OsO_4 solution was used for postfixation as previously described (Mizoguchi et al., 2002). Deeply anesthetized mice were transcardially perfused with 1×

HBSS with Ca^{2+} and Mg^{2+} containing 10 mM HEPES, 1 mM sodium pyruvate, 4% sucrose, and 4% paraformaldehyde at room temperature for 7 min. The brains were soaked in the same fixative at 4°C for 4 h and then in the cacodylate-buffered solution containing 2 mM $CaCl_2$, 30% sucrose, and cOmplete Mini protease inhibitor cocktail tablets (Roche Diagnostics) at 4°C overnight. For postfixation, 0.5% OsO_4 solution was used. The ultrathin sections were viewed by the JEOL 1011 electron microscopy (JEOL, Tokyo, Japan).

2.8. Statistical analysis

Statistical analysis of the difference between two mean values was performed with the two-tailed Student's *t*-test. The criterion for statistical significance was set at $p < 0.05$. All values are reported as the mean ± s.e.m.

3. Results

3.1. In vitro interaction of nectin-2α with DPP6, but not with Kv4.2 or KChIP1

We first examined by an immunoprecipitation assay whether nectin-2α interacts with Kv4.2, DPP6, or KChIP1. Either HA-tagged Kv4.2, HA-tagged DPP6, or HA-tagged KChIP1 was co-expressed with FLAG-tagged nectin-2α in HEK293E cells. The cell lysates were separately prepared and FLAG-tagged nectin-2α was immunoprecipitated with the FLAG-tagged protein purification gel from the respective cell lysates. HA-Tagged DPP6, but not HA-tagged Kv4.2 or HA-tagged KChIP1, was co-immunoprecipitated with FLAG-tagged nectin-2α (Fig. 2A, arrowheads). Conversely, when FLAG-tagged nectin-2α was co-expressed with either HA-tagged Kv4.2, HA-tagged DPP6, or HA-tagged KChIP1 in HEK293E cells and the respective HA-tagged proteins were immunoprecipitated with the HA-tagged protein purification gel from the respective cell lysates, FLAG-tagged nectin-2α was co-immunoprecipitated with HA-tagged DPP6, but not with HA-tagged

Kv4.2 or HA-tagged KChIP1 (Fig. 2B). These results indicate that nectin-2α interacts with DPP6, but not with Kv4.2 or KChIP1 *in vitro*.

3.2. Interaction of nectin-2α with DPP6 through their extracellular regions

We then examined which region of nectin-2α, the extracellular or cytoplasmic region, interacts with DPP6. When HA-tagged DPP6 was co-expressed with FLAG-tagged full-length nectin-2α (FLAG-nectin-2α), nectin-2α mutant lacking the cytoplasmic region (FLAG-nectin-2α–ΔCP), or nectin-2α mutant lacking the extracellular region (FLAG-nectin-2α–ΔEC) in HEK293E cells and immunoprecipitated with the HA-tagged protein purification gel, FLAG-tagged full-length nectin-2α and nectin-2α–ΔCP, but not nectin-2α–ΔEC, were co-immunoprecipitated with HA-tagged DPP6 (Fig. 3, arrowheads and brackets). These results indicate that nectin-2α interacts with DPP6 through their extracellular regions.

3.3. Immunofluorescence microscopic colocalization of nectin-2a with DPP6 at the boundary between the adjacent somata of the clustered cholinergic neurons in the MHb

We then examined whether nectin-2α is colocalized with DPP6 at the boundary between the adjacent somata of the clustered cholinergic neurons in the MHb of the adult mouse at P56. Consistent with the previous observations (Shiotani et al., 2018), the immunofluorescence signal for nectin-2α was observed as a linear pattern at the boundary between the adjacent somata of the clustered cholinergic neurons (Fig. 4). The signal for DPP6 was also observed as a linear pattern at this boundary at least in the MHbI and MHbCv. The signals for nectin-2α and DPP6 were frequently colocalized with each other at these boundaries (Fig. 4, arrows). The average ratios of the three patterns in three independent experiments were 55.6 ± 4.5% for the linear signal in which nectin-2α and DPP6 were colocalized, 21.8 ± 3.6% for the linear signal in which nectin-2α, but not DPP6, was localized, and 22.6 ± 1.2% for the linear signal in which DPP6, but not nectin-2α, was localized in the MHbI (two different specimens from each of three wild-type mice were

analyzed). Essentially, the same results were obtained in the MHbCv (data not shown). Thus, nectin-2α is frequently colocalized with DPP6 at the boundary between the adjacent somata of the clustered cholinergic neurons in the MHbI and the MHbCv of the adult MHb, although either nectin-2α alone or DPP6 alone is less frequently observed at this boundary. These results indicate that nectin-2α is apparently colocalized with DPP6 at the boundary between the adjacent somata of the clustered cholinergic neurons in the MHbI and the MHbCv.

3.4. No effect of genetic ablation of nectin-2 on the localization of DPP6 at the boundary between the adjacent somata of cholinergic neurons in the developing and adult MHbs

We previously showed that the immunofluorescence signal for Kv4.2 at the boundary between the adjacent somata of the clustered cholinergic neurons in the adult MHbs of the *nectin-2*-deficient mice at P56 is not different from that in the adult MHbs of the *nectin-2*-heterozygous mice at P56, whereas that in the developing MHbs of the *nectin-2*-deficient mice at P14 and P28 is markedly reduced, compared with that in the developing MHb of the *nectin-2*-heterozygous mice at P14 and P28 (Shiotani et al., 2018). However, at P56, the signal for DPP6 at the boundary between the adjacent neuronal somata in MHbI and MHbCv of the wild-type mouse was observed in 57.1 ± 0.9% cells, whereas that of the *nectin-2*-deficient mouse was observed in 57.4 ± 2.1% cells (Fig. 5A, B, and E). At P14, the signal for DPP6 at the boundary between the adjacent neuronal somata in the primordial region for the MHbCv, the MHbL, and the lateral part of the MHbI of the control *nectin-2*-heterozygous mouse was observed in 43.7 ± 2.3% cells, whereas that of the *nectin-2*-deficient mouse was observed in 42.1 ± 3.2% cells (Fig. 5C–E). Thus, the signals for DPP6 at the boundary between the adjacent somata of the cholinergic neurons in the MHbs of the *nectin-2*-deficient mice at P56 and P14 were not different from that in the MHbs of the control mice (Fig. 5E). These results indicate that nectin-2α is not essential for the localization of DPP6 at the boundary between the adjacent somata of the clustered cholinergic neurons in the adult and developing MHbs, although nectin-2α enhances the localization of Kv4.2 in the developing MHb (Shiotani et al., 2018).

3.5. Immunoelectron microscopical localization of DPP6 at the MSs of the clustered cholinergic neurons in the MHb

We then determined the precise localization of DPP6 at the boundary between the adjacent somata of the clustered cholinergic neurons in the MHbI of the adult MHb of mice at P56 by immunoelectron microscopy. For this purpose, the anti-DPP6 pAb which recognizes the extracellular region of DPP6 was used. The immunogold particles for DPP6 were observed at the intercellular space of the apposed plasma membranes (Fig. 6, arrows). They were observed often at the edge and occasionally at the outside of the MSs. Together with the previous observations (Kollo et al., 2006; Shiotani et al., 2018), these results suggest that DPP6 is partly colocalized with nectin-2α at the outside of the MSs and partly colocalized with Kv4.2 at the MSs.

4. Discussion

DPP6 (alias, DPPX) is a type-II transmembrane protein composed of a large extracellular carboxyl-terminal domain, a single transmembrane domain, and a short amino-terminal domain, which is alternatively spliced (Kin et al., 2001; Nadal et al., 2003). Although DPP6 has a serine aminopeptidase domain in the extracellular domain, DPP6 lacks enzymatic activity (Kin et al., 2001). We showed here that nectin-2α interacted with DPP6, but not with Kv4.2 or KChIP1, through their extracellular regions *in vitro*. It was previously shown that DPP6 and KChIP1 are the auxiliary components of Kv4.2 (An et al., 2000; Nadal et al., 2003). The present results together with these earlier observations suggest that nectin-2α binds to DPP6 and regulates the formation of the DPP6–Kv4.2–KChIP1 complex, and that nectin-2α regulates the functions of Kv4.2 through DPP6.

We then showed here that the immunofluorescence signal for DPP6 was co-concentrated with that for nectin-2α at the boundary between the adjacent somata of the clustered cholinergic neurons in the adult and developing MHbs. We previously showed that the immunogold particles for Kv4.2 are localized at the MSs, but that those for nectin-2α are localized on the apposed plasma membranes mostly at the outside of these

370 MSs, but occasionally localized at their edges and insides (Shiotani et al., 2018). We
371 showed here that the immunogold particles for DPP6 were localized on the apposed plasma
372 membranes at both the inside and the outside of the MSs. It has not been shown that both
373 Kv4.2 and DPP6 are localized at the MSs of the MHb, but the present and previous results
374 indicate that these two molecules form a complex and are localized at the MSs of the MHb.
375 It is not known whether nectin-2α *cis*-interacts with DPP6 *in vivo*, but the present and
376 previous results suggest that nectin-2α *cis*-interacts with DPP6 at the outside of the MSs in
377 the processes of the attachment of the somata of the clustered cholinergic neurons and the
378 formation of the MSs in the developing MHb (Fig. 1E).

379 It was previously shown that DPP6 is mainly expressed in the brain (Kin et al., 2001)
380 and that DPP6 and DPP10 enhance the localization of Kv4.2 on the plasma membrane in
381 cultured HEK293 cells (Foeger et al., 2012). We previously showed that the localization of
382 Kv4.2 is markedly reduced at the boundary between the adjacent somata of the clustered
383 cholinergic neurons in the developing MHb of the *nectin-2*-deficient mice at P14 and P28,
384 although this reduction is not observed in the *nectin-2*-deficient mice at P56, indicating that
385 nectin-2α is not essential for, but enhances the localization of Kv4.2 at the boundary
386 between the adjacent somata of the clustered cholinergic neurons in the developing MHb
387 (Shiotani et al., 2018). However, we showed here that the localization of DPP6 was not
388 changed at the boundary between the adjacent somata of the clustered cholinergic neurons
389 in the developing and adult MHbs of the *nectin-2*-deficient mice. These results indicate that
390 nectin-2α enhances the localization of Kv4.2 in a DPP6-independent manner at the
391 boundary between the adjacent somata of the clustered cholinergic neurons in the
392 developing MHbs.

393 The somata of neurons in the brain generally do not attach to each other. However, it
394 was shown that the unidentified neurons are clustered and that their somata are
395 exceptionally attached to each other directly in the MHb (Kollo et al., 2006). In addition, it
396 was shown that the Kv4.2-assocaited MSs are localized at the boundary between the
397 adjacent somata of these clustered neurons in the MHb (Kollo et al., 2006). We previously
398 showed that cholinergic neurons are clustered in the MHb (Shiotani et al., 2018). We
399 furthermore showed that the MSs are localized at the boundary between the adjacent
400 somata of the clustered cholinergic neurons and that the plasma membrane of the MSs is

401 darkened, compared with that of the regions other than the MSs (Shiotani et al., 2018).
402 These features of the MSs suggest that the MSs are likely to serve as a cell adhesion
403 apparatus that attaches these somata to each other, but its responsible CAM or its binding
404 protein has not been identified and the only molecule that is always associated with the
405 MSs is Kv4.2 (Kollo et al., 2006; Shiotani et al., 2018). However, Kv4.2 is mostly
406 distributed on the apposed plasma membranes in an asymmetrical manner against the
407 plasma membrane at the MSs (Kollo et al., 2006; Shiotani et al., 2018), suggesting that
408 Kv4.2 is not likely to serve as a CAM at the MSs. The previous result that the
409 immunofluorescence signal for Kv4.2 is reduced in the developing MHb of the
410 *nectin-2*-deficient mice at P14 and P28 suggests that the number and/or the length of the
411 MSs are reduced in the developing MHb of the *nectin-2*-deficient mice, although we did
412 not confirm by transmission electron microscopy or immunoelectron microscopy that the
413 number and/or the length of the MSs are indeed reduced in the developing MHb of the
414 *nectin-2*-deficient mice at P14 and P28. In contrast, the present results showed that the
415 immunofluorescence signal for the auxiliary protein of Kv4.2, DPP6, was not changed in
416 the developing and adult MHbs of the *nectin-2*-deficient mice, suggesting that DPP6 plays
417 a role other than the auxiliary protein of Kv4.2. DPP6 is localized at both the edge and the
418 outside of the MSs. Thus, it might be unlikely that DPP6 serves as a CAM at the MSs,
419 although further analysis is needed.

420 The previous results further showed that *nectin-2* is not required for the clustering of
421 the cholinergic neurons (Shiotani et al., 2018). Currently, it is not known why the
422 cholinergic neurons are clustered in the MHb, but it can be speculated that the clustering of
423 the cholinergic neurons is required for these neurons to fire synchronously. This unique
424 feature of these neurons in the MHb could be related to the unique physiological functions
425 of the MHb. Kv4.2 is a voltage-gated K^+ channel which produces the somatodendritic
426 subthreshold A-type current (I_{SA}) and attenuates the back-propagation of action potentials
427 in hippocampal pyramidal neurons (Jerng and Pfaffinger, 2014). Kv4.2 is also known to
428 form an ion channel complex with its auxiliary subunits, such as KChIPs and DPP6 (An et
429 al., 2000; Nadal et al., 2003). These auxiliary subunits change the properties of Kv4.2,
430 which exhibits fast inactivation and slow recovery from inactivation (Jerng and Pfaffinger,
431 2014). These characteristics of Kv4.2 could be suitable for the synchronization of the firing

of the clustered cholinergic neurons. Nectin-2α could regulate this process through DPP6. However, it is unknown why Kv4.2 is accumulated at the MSs or whether the MSs would regulate the accumulation of Kv4.2 during the activation of the cholinergic neurons in the MHb. Further analysis is required to resolve these issues.

Our previous series of studies showed that nectin first initiates cell-cell adhesion and then recruits cadherin to the nectin-based cell-cell adhesion sites through the nectin-binding protein afadin to adherens junctions in many types of cells including epithelial cells and fibroblasts (Tachibana et al., 2000; Takai et al., 2008a). In addition, nectin *cis*-interacts on the same plasma membrane with many growth factor receptors or integrins: nectin-1 *cis*-interacts with the FGF receptor (Bojesen et al., 2012) and integrin $\alpha_v\beta_3$ (Sakamoto et al., 2006); nectin-3 *cis*-interacts with the PDGF receptor (Kanzaki et al., 2008) and integrin $\alpha_v\beta_3$ (Sakamoto et al., 2006; Sakamoto et al., 2008); and nectin-4 *cis*-interacts with the prolactin receptor (Kitayama et al., 2016). In the *cis*-interaction of nectin-4 with the prolactin receptor, nectin-4 forms a spot with *trans*-interacting nectin-1 at the boundary between the luminal and basal cells in the mammary gland (Kitayama et al., 2016). We previously showed that the nectin-2α-mediated cell adhesion apparatus is similar to this nectin-1-4 spot (Shiotani et al., 2018). We showed here that nectin-2α directly interacted with DPP6, but not Kv4.2 or KChIP, at least *in vitro,* and that the localization of DPP6 was independent of nectin-2α, although we previously showed that the localization of Kv4.2 is partly dependent of nectin-2α (Shiotani et al., 2018). The mechanisms for the formation of the MSs, the recruitment of the Kv4.2–DPP6–KChIP1 complex to the MSs, and the role or mode of action of nectin-2α in these processes remain unknown, but the present and previous results collectively suggest that the MSs are formed by an unidentified CAM(s) and that DPP6 *cis*-interacts directly or indirectly with this CAM and is recruited to the MSs whereas nectin-2α *cis*-interacts with this DPP6 and regulates the formation of DPP6–Kv4.2–KChIP1 complex to recruit this complex to the MSs, eventually leading to the formation of the MSs and the attachment of the adjacent somata of the clustered cholinergic neurons in the developing MHb. After the formation of the MSs and the attachment of the adjacent somata of the clustered cholinergic neurons, Kv4.2 and DPP6 may be dissociated from each other or from nectin-2α to be localized at the different regions. The identification of the CAM(s) for the MSs would be critical to elucidate the mechanisms for the formation

463 of the MSs, the attachment of the adjacent somata of the cholinergic neurons, the
464 recruitment of the DPP6–Kv4.2–KChIP1 complex to the MSs, and the role or mode of
465 action of nectin-2α in these processes in the MHb.
466

Acknowledgments

This work was supported by JSPS KAKENHI Grant Number 26251013 (to Y.T.); and MEXT KAKENHI Grant Numbers 26114007 (Y.T.), 16H06461 (to A.M.), and 16H06463 (to K.Ma.).

References

Aizawa, H., Kobayashi, M., Tanaka, S., Fukai, T., Okamoto, H., 2012. Molecular characterization of the subnuclei in rat habenula. J Comp Neurol 520, 4051-4066.

An, W.F., Bowlby, M.R., Betty, M., Cao, J., Ling, H.P., Mendoza, G., Hinson, J.W., Mattsson, K.I., Strassle, B.W., Trimmer, J.S., Rhodes, K.J., 2000. Modulation of A-type potassium channels by a family of calcium sensors. Nature 403, 553-556.

Andres, K.H., von Düring, M., Veh, R.W., 1999. Subnuclear organization of the rat habenular complexes. J Comp Neurol 407, 130-150.

Aoki, J., Koike, S., Asou, H., Ise, I., Suwa, H., Tanaka, T., Miyasaka, M., Nomoto, A., 1997. Mouse homolog of poliovirus receptor-related gene 2 product, mPRR2, mediates homophilic cell aggregation. Exp Cell Res 235, 374-384.

Balcita-Pedicino, J.J., Omelchenko, N., Bell, R., Sesack, S.R., 2011. The inhibitory influence of the lateral habenula on midbrain dopamine cells: ultrastructural evidence for indirect mediation via the rostromedial mesopontine tegmental nucleus. J Comp Neurol 519, 1143-1164.

Birnbaum, S.G., Varga, A.W., Yuan, L.L., Anderson, A.E., Sweatt, J.D., Schrader, L.A., 2004. Structure and function of Kv4-family transient potassium channels. Physiol Rev 84, 803-833.

Bojesen, K.B., Clausen, O., Rohde, K., Christensen, C., Zhang, L., Li, S., Køhler, L., Nielbo, S., Nielsen, J., Gjørlund, M.D., Poulsen, F.M., Bock, E., Berezin, V., 2012. Nectin-1 binds and signals through the fibroblast growth factor receptor. J Biol Chem 287, 37420-37433.

Carlson, J., Noguchi, K., Ellison, G., 2001. Nicotine produces selective degeneration in the medial habenula and fasciculus retroflexus. Brain Res 906, 127-134.

Christoph, G.R., Leonzio, R.J., Wilcox, K.S., 1986. Stimulation of the lateral habenula inhibits dopamine-containing neurons in the substantia nigra and ventral tegmental area of the rat. J Neurosci 6, 613-619.

Cuello, A.C., Emson, P.C., Paxinos, G., Jessell, T., 1978. Substance P containing and cholinergic projections from the habenula. Brain Res 149, 413-429.

Eberlé, F., Dubreuil, P., Mattei, M.G., Devilard, E., Lopez, M., 1995. The human PRR2 gene, related to the human poliovirus receptor gene (PVR), is the true homolog of the murine MPH gene. Gene 159, 267-272.

Foeger, N.C., Norris, A.J., Wren, L.M., Nerbonne, J.M., 2012. Augmentation of Kv4.2-encoded currents by accessory dipeptidyl peptidase 6 and 10 subunits reflects selective cell surface Kv4.2 protein stabilization. J Biol Chem 287, 9640-9650.

Groenewegen, H.J., Ahlenius, S., Haber, S.N., Kowall, N.W., Nauta, W.J., 1986. Cytoarchitecture, fiber connections, and some histochemical aspects of the interpeduncular nucleus in the rat. J Comp Neurol 249, 65-102.

Harold, D., Abraham, R., Hollingworth, P., Sims, R., Gerrish, A., Hamshere, M.L., Pahwa, J.S., Moskvina, V., Dowzell, K., Williams, A., Jones, N., Thomas, C., Stretton, A., Morgan, A.R., Lovestone, S., Powell, J., Proitsi, P., Lupton, M.K., Brayne, C., Rubinsztein, D.C., Gill, M., Lawlor, B., Lynch, A., Morgan, K., Brown, K.S., Passmore, P.A., Craig, D., McGuinness, B., Todd, S., Holmes, C., Mann, D., Smith, A.D., Love, S., Kehoe, P.G., Hardy, J., Mead, S., Fox, N., Rossor, M., Collinge, J., Maier, W., Jessen, F., Schurmann, B.,

Heun, R., van den Bussche, H., Heuser, I., Kornhuber, J., Wiltfang, J., Dichgans, M., Frölich, L., Hampel, H., Hüll, M., Rujescu, D., Goate, A.M., Kauwe, J.S., Cruchaga, C., Nowotny, P., Morris, J.C., Mayo, K., Sleegers, K., Bettens, K., Engelborghs, S., De Deyn, P.P., Van Broeckhoven, C., Livingston, G., Bass, N.J., Gurling, H., McQuillin, A., Gwilliam, R., Deloukas, P., Al-Chalabi, A., Shaw, C.E., Tsolaki, M., Singleton, A.B., Guerreiro, R., Mühleisen, T.W., Nöthen, M.M., Moebus, S., Jöckel, K.H., Klopp, N., Wichmann, H.E., Carrasquillo, M.M., Pankratz, V.S., Younkin, S.G., Holmans, P.A., O'Donovan, M., Owen, M.J., Williams, J., 2009. Genome-wide association study identifies variants at CLU and PICALM associated with Alzheimer's disease. Nat Genet 41, 1088-1093.

Herkenham, M., Nauta, W.J., 1977. Afferent connections of the habenular nuclei in the rat. A horseradish peroxidase study, with a note on the fiber-of-passage problem. J Comp Neurol 173, 123-146.

Herkenham, M., Nauta, W.J., 1979. Efferent connections of the habenular nuclei in the rat. J Comp Neurol 187, 19-47.

Jerng, H.H., Pfaffinger, P.J., 2014. Modulatory mechanisms and multiple functions of somatodendritic A-type K (+) channel auxiliary subunits. Front Cell Neurosci 8, 82.

Kanzaki, N., Ogita, H., Komura, H., Ozaki, M., Sakamoto, Y., Majima, T., Ijuin, T., Takenawa, T., Takai, Y., 2008. Involvement of the nectin-afadin complex in PDGF-induced cell survival. J Cell Sci 121, 2008-2017.

Kin, Y., Misumi, Y., Ikehara, Y., 2001. Biosynthesis and characterization of the brain-specific membrane protein DPPX, a dipeptidyl peptidase IV-related protein. J Biochem 129, 289-295.

Kitayama, M., Mizutani, K., Maruoka, M., Mandai, K., Sakakibara, S., Ueda, Y., Komori, T., Shimono, Y., Takai, Y., 2016. A Novel Nectin-mediated Cell Adhesion Apparatus That Is Implicated in Prolactin Receptor Signaling for Mammary Gland Development. J Biol Chem 291, 5817-5831.

Kobayashi, Y., Sano, Y., Vannoni, E., Goto, H., Suzuki, H., Oba, A., Kawasaki, H., Kanba, S., Lipp, H.P., Murphy, N.P., Wolfer, D.P., Itohara, S., 2013. Genetic dissection of medial habenula-interpeduncular nucleus pathway function in mice. Front Behav Neurosci 7, 17.

Kollo, M., Holderith, N.B., Nusser, Z., 2006. Novel subcellular distribution pattern of A-type K+ channels on neuronal surface. J Neurosci 26, 2684-2691.

Logue, M.W., Schu, M., Vardarajan, B.N., Buros, J., Green, R.C., Go, R.C., Griffith, P., Obisesan, T.O., Shatz, R., Borenstein, A., Cupples, L.A., Lunetta, K.L., Fallin, M.D., Baldwin, C.T., Farrer, L.A., Multi-Institutional Research on Alzheimer Genetic Epidemiology Study, G., 2011. A comprehensive genetic association study of Alzheimer disease in African Americans. Arch Neurol 68, 1569-1579.

Mathuru, A.S., Jesuthasan, S., 2013. The medial habenula as a regulator of anxiety in adult zebrafish. Front Neural Circuits 7, 99.

Miyata, M., Mandai, K., Maruo, T., Sato, J., Shiotani, H., Kaito, A., Itoh, Y., Wang, S., Fujiwara, T., Mizoguchi, A., Takai, Y., Rikitake, Y., 2016. Localization of nectin-2delta at perivascular astrocytic endfoot processes and degeneration of astrocytes and neurons in nectin-2 knockout mouse brain. Brain Res 1649, 90-101.

Mizoguchi, A., Nakanishi, H., Kimura, K., Matsubara, K., Ozaki-Kuroda, K., Katata, T., Honda, T., Kiyohara, Y., Heo, K., Higashi, M., Tsutsumi, T., Sonoda, S., Ide, C., Takai, Y., 2002. Nectin: an adhesion molecule involved in formation of synapses. J Cell Biol 156, 555-565.

Molas, S., DeGroot, S.R., Zhao-Shea, R., Tapper, A.R., 2017. Anxiety and Nicotine

Dependence: Emerging Role of the Habenulo-Interpeduncular Axis. Trends Pharmacol Sci 38, 169-180.
Morrison, M.E., Racaniello, V.R., 1992. Molecular cloning and expression of a murine homolog of the human poliovirus receptor gene. J Virol 66, 2807-2813.
Mueller, S., Rosenquist, T.A., Takai, Y., Bronson, R.A., Wimmer, E., 2003. Loss of nectin-2 at Sertoli-spermatid junctions leads to male infertility and correlates with severe spermatozoan head and midpiece malformation, impaired binding to the zona pellucida, and oocyte penetration. Biol Reprod 69, 1330-1340.
Nadal, M.S., Ozaita, A., Amarillo, Y., Vega-Saenz de Miera, E., Ma, Y., Mo, W., Goldberg, E.M., Misumi, Y., Ikehara, Y., Neubert, T.A., Rudy, B., 2003. The CD26-related dipeptidyl aminopeptidase-like protein DPPX is a critical component of neuronal A-type K+ channels. Neuron 37, 449-461.
Nishikawa, T., Fage, D., Scatton, B., 1986. Evidence for, and nature of, the tonic inhibitory influence of habenulointerpeduncular pathways upon cerebral dopaminergic transmission in the rat. Brain Res 373, 324-336.
Nishikawa, T., Scatton, B., 1985. Inhibitory influence of GABA on central serotonergic transmission. Involvement of the habenulo-raphe pathways in the GABAergic inhibition of ascending cerebral serotonergic neurons. Brain Res 331, 81-90.
Ozaki-Kuroda, K., Nakanishi, H., Ohta, H., Tanaka, H., Kurihara, H., Mueller, S., Irie, K., Ikeda, W., Sakai, T., Wimmer, E., Nishimune, Y., Takai, Y., 2002. Nectin couples cell-cell adhesion and the actin scaffold at heterotypic testicular junctions. Curr Biol 12, 1145-1150.
Qin, C., Luo, M., 2009. Neurochemical phenotypes of the afferent and efferent projections of the mouse medial habenula. Neuroscience 161, 827-837.
Sakamoto, Y., Ogita, H., Hirota, T., Kawakatsu, T., Fukuyama, T., Yasumi, M., Kanzaki, N., Ozaki, M., Takai, Y., 2006. Interaction of integrin alpha(v)beta3 with nectin. Implication in cross-talk between cell-matrix and cell-cell junctions. J Biol Chem 281, 19631-19644.
Sakamoto, Y., Ogita, H., Komura, H., Takai, Y., 2008. Involvement of nectin in inactivation of integrin alpha(v)beta(3) after the establishment of cell-cell adhesion. J Biol Chem 283, 496-505.
Shiotani, H., Miyata, M., Itoh, Y., Wang, S., Kaito, A., Mizoguchi, A., Yamasaki, M., Watanabe, M., Mandai, K., Mochizuki, H., Takai, Y., 2018. Localization of nectin-2alpha at the boundary between the adjacent somata of the clustered cholinergic neurons and its regulatory role in the subcellular localization of the voltage-gated A-type K(+) channel Kv4.2 in the medial habenula. J Comp Neurol 526, 1527-1549.
Shumake, J., Edwards, E., Gonzalez-Lima, F., 2003. Opposite metabolic changes in the habenula and ventral tegmental area of a genetic model of helpless behavior. Brain Res 963, 274-281.
Tachibana, K., Nakanishi, H., Mandai, K., Ozaki, K., Ikeda, W., Yamamoto, Y., Nagafuchi, A., Tsukita, S., Takai, Y., 2000. Two cell adhesion molecules, nectin and cadherin, interact through their cytoplasmic domain-associated proteins. J Cell Biol 150, 1161-1176.
Takahashi, K., Nakanishi, H., Miyahara, M., Mandai, K., Satoh, K., Satoh, A., Nishioka, H., Aoki, J., Nomoto, A., Mizoguchi, A., Takai, Y., 1999. Nectin/PRR: an immunoglobulin-like cell adhesion molecule recruited to cadherin-based adherens junctions through interaction with Afadin, a PDZ domain-containing protein. J Cell Biol 145, 539-549.
Takai, Y., Ikeda, W., Ogita, H., Rikitake, Y., 2008a. The immunoglobulin-like cell adhesion molecule nectin and its associated protein afadin. Annu Rev Cell Dev Biol 24, 309-342.
Takai, Y., Miyoshi, J., Ikeda, W., Ogita, H., 2008b. Nectins and nectin-like molecules: roles

in contact inhibition of cell movement and proliferation. Nat Rev Mol Cell Biol 9, 603-615.
Takei, N., Miyashita, A., Tsukie, T., Arai, H., Asada, T., Imagawa, M., Shoji, M., Higuchi, S., Urakami, K., Kimura, H., Kakita, A., Takahashi, H., Tsuji, S., Kanazawa, I., Ihara, Y., Odani, S., Kuwano, R., Japanese Genetic Study Consortium for Alzheimer, D., 2009. Genetic association study on in and around the APOE in late-onset Alzheimer disease in Japanese. Genomics 93, 441-448.
Toyoshima, D., Mandai, K., Maruo, T., Supriyanto, I., Togashi, H., Inoue, T., Mori, M., Takai, Y., 2014. Afadin regulates puncta adherentia junction formation and presynaptic differentiation in hippocampal neurons. PLoS One 9, e89763.
Wang, R.Y., Aghajanian, G.K., 1977. Physiological evidence for habenula as major link between forebrain and midbrain raphe. Science 197, 89-91.
Warner, M.S., Geraghty, R.J., Martinez, W.M., Montgomery, R.I., Whitbeck, J.C., Xu, R., Eisenberg, R.J., Cohen, G.H., Spear, P.G., 1998. A cell surface protein with herpesvirus entry activity (HveB) confers susceptibility to infection by mutants of herpes simplex virus type 1, herpes simplex virus type 2, and pseudorabies virus. Virology 246, 179-189.

Figures and Figure legends

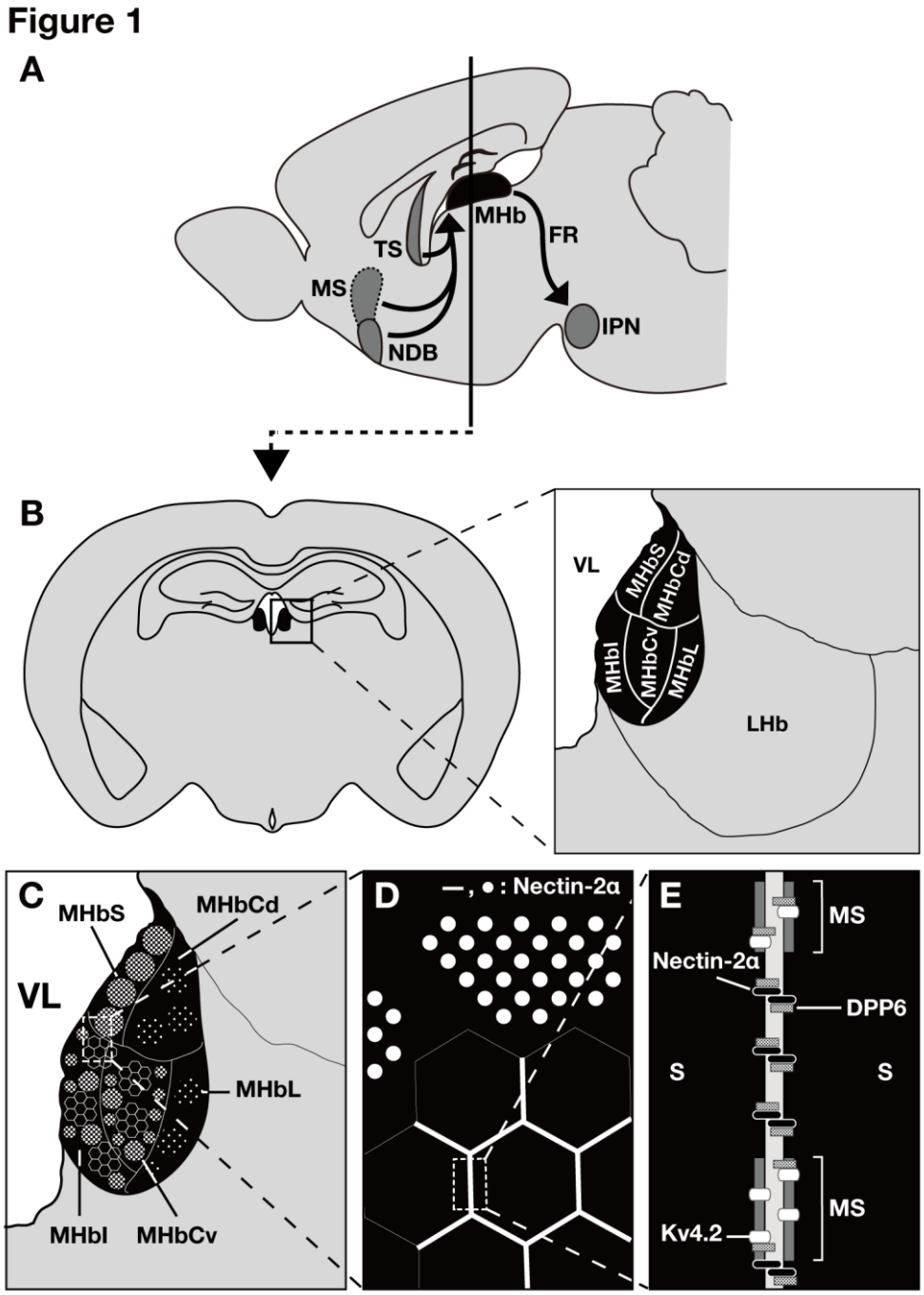

Fig. 1. Schematic drawings of the habenula in the adult mouse brain and the localization of nectin-2α, Kv4.2, and DPP6. (A) A sagittal view. MHb, the medial habenula; MS, the

medial septum; NDB, the nucleus of diagonal band; TS, the triangular septum; FR, the fasciculus retroflexus; and IPN, the interpeduncular nucleus. (B) The habenula. A coronal view at the indicated rostrocaudal level in (A). The encircled area in the left panel is highlighted in the right panel. The habenula consists of the MHb and the lateral habenula (LHb). The MHb is divided into five subregions: the MHbS, the MHbI, the MHbCd, the MHbCv, and the MHbL. VL, the third ventricle. (C–E) Localization of nectin-2α, Kv4.2, and DPP6 in the MHb. (C) A high magnification image of the encircled area in (B). (D) A high magnification image of the encircled area in (C). The white punctates in (C, D) and bold lines in (D) indicate neuronal expression of nectin-2α with a punctate pattern and a liner pattern, respectively. (E) A high magnification image of the encircled area in (D). S, somata of the cholinergic neurons; and MS, the membrane specialization. This figure was modified from Figure 1 in the previous paper (Shiotani et al., 2018).

Figure 2

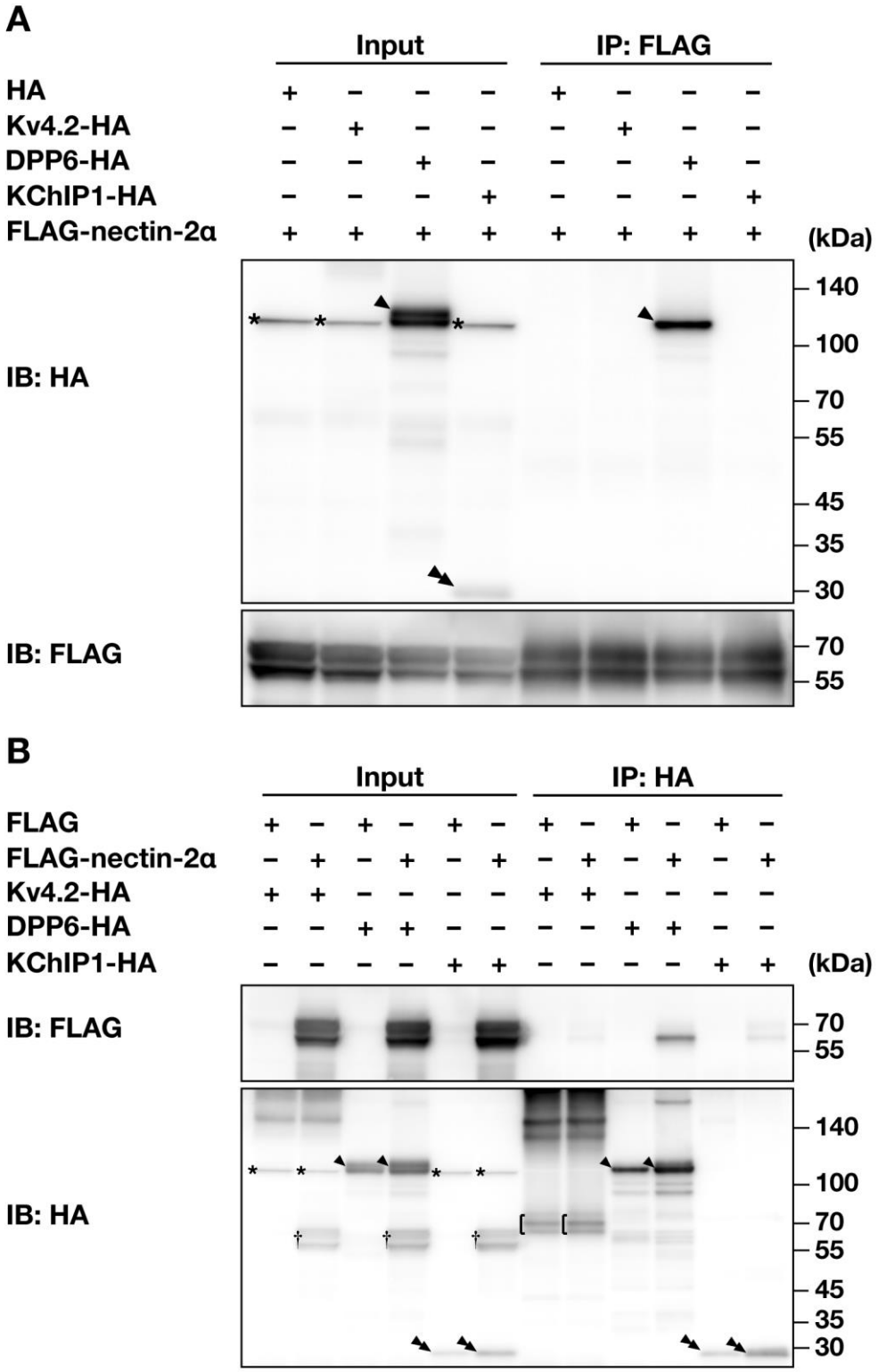

647

648

649 **Fig. 2.** Interaction of nectin-2α with DPP6, but not with Kv4.2 or KChIP1. (A)
650 Co-immunoprecipitation of DPP6 with nectin-2α. HEK293E cells were transfected with
651 FLAG-tagged nectin-2α in combination with either HA-tagged Kv4.2, HA-tagged DPP6,
652 or HA-tagged KChIP1. FLAG-Tagged nectin-2α was immunoprecipitated with the
653 FLAG-tagged protein purification gel from the respective cell lysates. The precipitates were
654 subjected to Western blotting using the indicated Abs. (B) Co-immunoprecipitation of
655 nectin-2α with DPP6. HEK293E cells were transfected with FLAG-tagged nectin-2α in
656 combination with either HA-tagged Kv4.2, HA-tagged DPP6, or HA-tagged KChIP1. The
657 respective HA-tagged proteins were immunoprecipitated with the HA-tagged protein
658 purification gel from the respective cell lysates. The precipitates were subjected to Western
659 blotting using the indicated Abs. IB, immunoblotting; and IP, immunoprecipitation.
660 Arrowheads, DPP6-HA; double arrowheads, KChIP1-HA; brackets, Kv4.2-HA; asterisks,
661 non-specific bands; and daggers, non-specific bands caused by re-blotting of the membrane.
662 The results shown are the representative of three independent experiments.

Figure 3

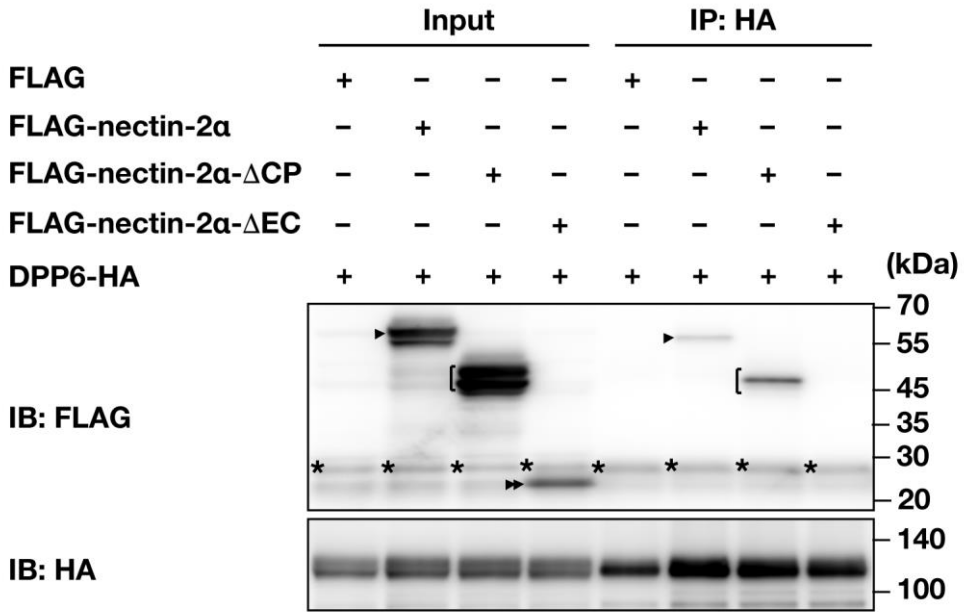

Fig. 3. Interaction of nectin-2α with DPP6 through their extracellular regions. HEK293E cells were transfected with HA-tagged DPP6 in combination with either FLAG-tagged full-length nectin-2α (FLAG-nectin-2α), FLAG-tagged nectin-2α mutant lacking the cytoplasmic region (FLAG-nectin-2α–ΔCP), or FLAG-tagged nectin-2α mutant lacking the extracellular region (FLAG-nectin-2α–ΔEC). HA-Tagged DPP6 was immunoprecipitated with the HA-tagged protein purification gel from the respective cell lysates. The precipitates were subjected to Western blotting using the indicated Abs. IB, immunoblotting; and IP, immunoprecipitation. Arrowheads, FLAG-nectin-2α; brackets, FLAG-nectin-2α–ΔCP; double arrowhead, FLAG-nectin-2α–ΔEC; and asterisks, non-specific bands. The results shown are the representative of three independent experiments.

Figure 4

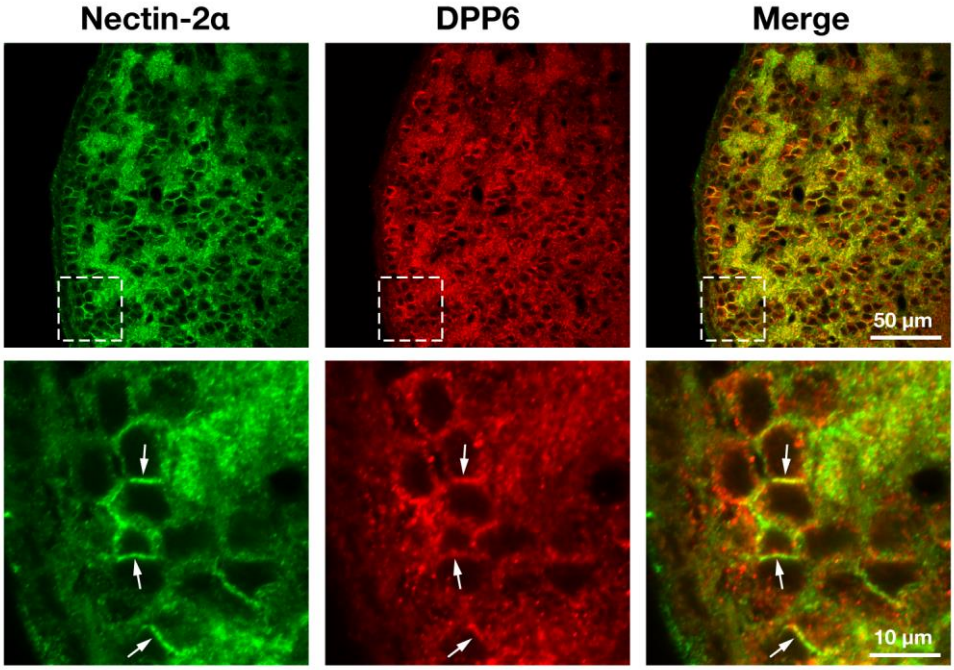

Fig. 4. Colocalization of nectin-2α with DPP6 at the boundary between the adjacent somata of the clustered cholinergic neurons in the MHbI. Double immunofluorescence images for nectin-2α and DPP6 in the MHbI of the wild-type mice at P56. Immunofluorescence microscopy was performed using the indicated Abs. The encircled region in the upper panel is highlighted in the lower panel. Arrows, the areas where the signals for both nectin-2α and DPP6 with the linear pattern were observed. The results shown are representative of three independent experiments.

Figure 5

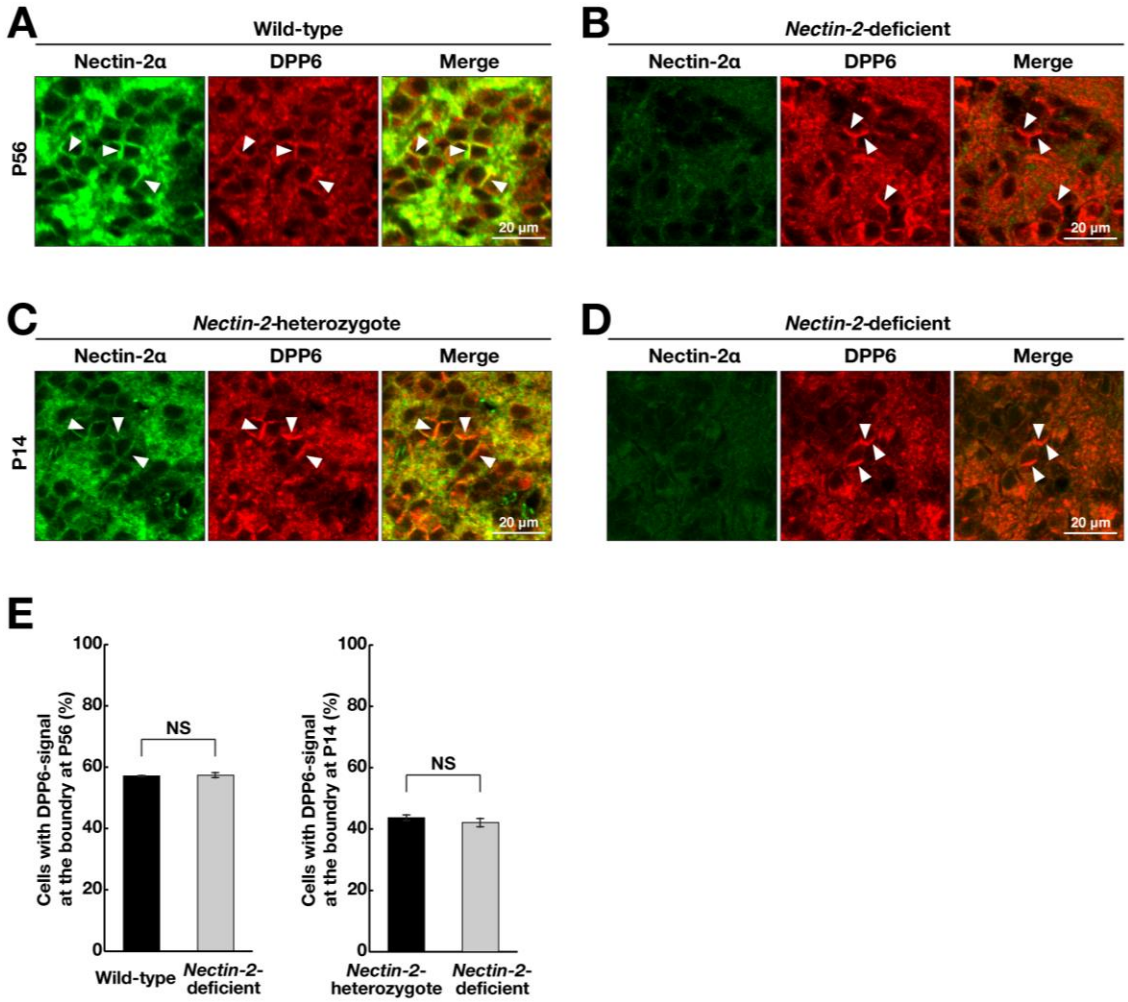

Fig. 5. No requirement of *nectin-2* for the localization of DPP6 at the boundary between the adjacent somata of the clustered cholinergic neurons in the MHb. Immunofluorescence microscopy was performed using wild-type, *nectin-2*-heterozygous, and *nectin-2*-deficient mice at P56 and P14. (A–D) The immunofluorescence signals for nectin-2α and DPP6. The anti-nectin-2α/δ mAb and the anti-DPP6 pAb were used. (A, B) MHbI and MHbCv at P56. (C, D) The primordial region for the MHbCv, the MHbL, and the lateral part of the MHbI at P14. (A) The MHb of the wild-type mice. (B, D) The MHb of the *nectin-2*-deficient mice. (C) The MHb of the *nectin-2*-heterozygous mice. Arrowheads, the areas where the signal for DPP6 was observed at the boundary between the adjacent somata of the cholinergic neurons. (E) The average percentage of cells with the signal for DPP6 at the boundary

696 between the adjacent neuronal somata in MHbI and MHbCv at P56 and in the primordial
697 regions for the MHbCv, the MHbL, and the lateral part of the MHbI at P14. Two different
698 specimens from each of the three mice for each genotype were analyzed. NS, not
699 significant.

Figure 6

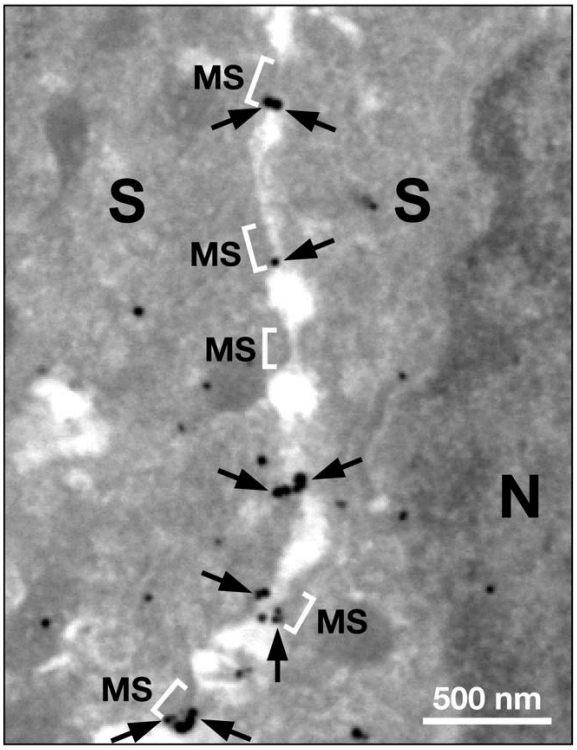

Fig. 6. Ultrastructural localization of DPP6 at the boundary between the adjacent somata of the clustered cholinergic neurons in the MHbI of the adult MHb. Immunoelectron microscopy was performed using the wild-type mouse at P56. The anti-DPP6 pAb that recognized the extracellular region of DPP6 was used. Arrows, the immunogold particles for DPP6. N, nucleus of a neuron; S, somata of neurons; MS, the membrane specialization. The result shown is representative of two independent experiments.